



# Assessment of spatial distribution of contaminants and their levels in soil and water resources of Calabar, Nigeria using geophysical and geological data

Anthony E. Akpan<sup>1</sup> · A. N. Ugbaja<sup>2</sup> · E. I. Okoyeh<sup>3</sup> · N. J. George<sup>4</sup>

Received: 2 December 2016 / Accepted: 19 December 2017 / Published online: 29 December 2017  
© Springer-Verlag GmbH Germany, part of Springer Nature 2017

## Abstract

The contamination levels of soils and water resources in Calabar, Nigeria have been investigated using resistivity (vertical electrical sounding and electrical resistivity tomography), geochemical analyses of soil and water resources and textural analysis. Sixty randomly sited VES sites were investigated in two seasons while ERT investigations were performed along four profiles. The geochemical investigations were spread across seasons in order to track seasonal changes in physico-chemical parameters: hydrogen ion concentration (pH), electrical conductivity, total dissolved solids, chloride ion ( $\text{Cl}^-$ ), nitrate ion ( $\text{NO}_3^-$ ), bicarbonate ( $\text{HCO}_3^-$ ), sulphate ion ( $\text{SO}_4^{2-}$ ), calcium ion ( $\text{Ca}^{2+}$ ), sodium ion ( $\text{Na}^+$ ), potassium ion ( $\text{K}^+$ ) and magnesium ion ( $\text{Mg}^{2+}$ ). Additionally, concentrations of ammonium, aluminium and nitrite ions in soils were determined. Results show that ionic concentrations in the sand-dominated soils and water are within permissible limits and baseline standards. The resistivities follow known trends in the area. However, at the central waste disposal site, a localised thin (< 5 m), low resistivity (< 15  $\Omega\text{m}$ ) anomaly suspected to be due to contamination by leachates was observed. Comparatively, the contaminated area is also characterised by marginal increase in ionic concentrations. Strong attenuation capacities of overlying and adjoining clay/lateritic sediments and optimal design of the waste dump site probably reduced the spread of contaminants. The contaminated zone need to be closely monitored so that it does not extend to the aquifers. Hence, all strategies presently being used in managing wastes in Calabar should be sustained.

**Keywords** Resistivity · Soil · Water · Environment · Contaminants · Calabar-Nigeria

## Introduction

Many towns in developing countries including Calabar in southeastern Nigeria have been struggling to cope with huge challenges posed by uncontrolled urbanisation and rapid industrialisation to both human and environment healths. Wide disparity still exists between demand and

supply of some basic socio-infrastructure facilities (e.g. potable water, food, hospital and road) needed to sustain the essential needs of a booming population (Neves and Morales 2007). Consequently, available resources are overstretched by this sudden and unplanned increase in demand. Just like in other climes, many service providers like farmers have promptly responded to the resulting scenario by adopting all manners of soil productivity and yield enhancement techniques to enhance the quantity of their products. These practices include excessive application of both organic and inorganic fertilizers: urea and NPK [i.e. nitrogen (15%), phosphorus (30%) and potassium (55%)], composts, pesticides, herbicides and soil fumigants. Such practices, particularly when performed in continuous and excessive manner, can harm both environmental and human healths (Yang et al. 2006; Hargreaves et al. 2008; Islami et al. 2011). Additionally, large quantities of wastes (municipal, agricultural and industrial), which are either dumped in a central waste dump site (WDS) located in

✉ Anthony E. Akpan  
anthonyakpan@yahoo.com; anthonyakpan@unical.edu.ng

<sup>1</sup> Applied Geophysics Programme, University of Calabar, PMB 1115, Calabar, Cross River State, Nigeria

<sup>2</sup> Geology Department, University of Calabar, PMB 1115, Calabar, Cross River State, Nigeria

<sup>3</sup> Geological Science Department, Nnamdi Azikiwe University, Awka, Anambra State, Nigeria

<sup>4</sup> Physics Department, Akwa Ibom State University, Ikot Akpaden, Mkpato Enin LGA, Akwa Ibom State, Nigeria

the northeastern part of Calabar (Fig. 1b–d) or repeatedly used as compost manure, are generated daily (Hargreaves et al. 2008). Furthermore, harmful gases and other industrial emissions are discharged continuously into our beleaguered environment (Loska et al. 2004; Orisakwe et al. 2004). The solid wastes are dominated by food and other remains of organic materials, paper and paper-based products, chemical and chemical products, metal and allied products, glasses, wood and wood products, textiles and rugs, rubber and rubber products, leather, plastics, earth, ash, cinder and construction rubbles.

Continuous discharge of these wastes into soils can lead to the accumulation of their trace element constituents (Krishna and Govil 2007). Continuous accretion of such elements in soils will eventually cause them to increase beyond their threshold levels. Such conditions portend dangerous consequences to public health, especially, in populated cities like Calabar. The soils, which are the main receptacles of these wastes, are not only the medium through which plants, which absorb these elements, grow, but are also that important interface that intrinsically connects the other components of the physical environment: air, plant and water.

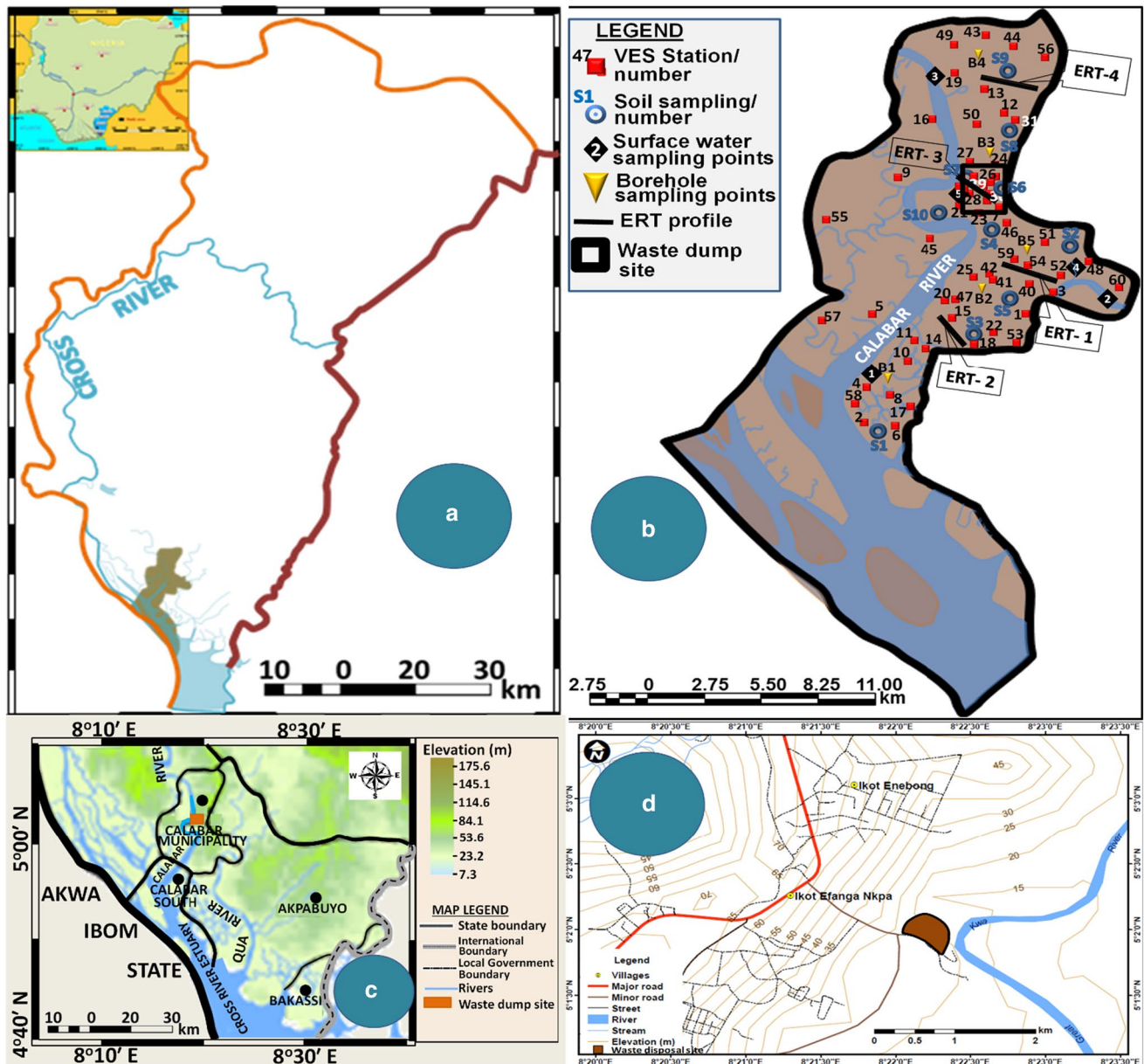


Fig. 1 Map of Cross River State **a** showing the location of the study area, map of Calabar, **b** showing water and soil sampling, and resistivity survey points, topographic map of southern Cross River State,

**c** showing the location of the study area and **d** elevation map around the waste dump site

Thus, the widespread practice of dumping toxic substances in soils is also an indirect way of transmitting them to the other components of the environment (Chen et al. 1999). Such transmissions, particularly in sand-dominated soils, can be enhanced by some natural and anthropogenic activities like combustion, wind transport, extraction and processing (for atmospheric environment); surface run-offs, wind transports, leakages from storage and sewage facilities for surface water resources, SWR (e.g. rivers, streams, ponds and lakes), soils and plants; and leaching, storage and mining facilities (for groundwater).

The consequences of environmental contamination, particularly from wastes, are currently very topical issues that environmentalists, environmental protection agencies and other concerned stakeholders in Calabar are not only discussing but are also working vigorously to prevent. This is because, even at the landfill site, contamination of soil and water resources, mainly by leachates, can still occur if it is not properly managed (Kanmani and Gandhimathi 2013; Fernández et al. 2014). This calls for closer monitoring of both active and abandoned WDSs. Otherwise, if they contaminate the soil and water resources, grievous consequences like reduction in soil productivity (Orisakwe et al. 2004; Yang et al. 2006) and hygienic quality of food (Bhattacharya et al. 2010; Lehto et al. 2011); degradation in drinking water quality (Almasri and Kaluarachchi 2004; Yang et al. 2006); air quality (D'Amato et al. 2010; Sartelet et al. 2012) and general decrease in physical, mental and environmental healths can occur. Although sustained enlightenment and sensitisation campaigns mounted by relevant governmental and non-governmental agencies have made many residents to be mindful of the dangers associated with environmental pollution, and necessary steps are being taken to minimise them, pockets of inappropriate waste disposal practices still persist in many locations. Excepting the biodegradable wastes, which are sometimes disposed inappropriately by residents, established polluting activities like excessive application of inorganic fertilizers like urea and NPK [i.e. nitrogen (15%), phosphorus (30%) and potassium (55%)], oil spills and other hydrocarbon exploitation, transportation and marketing activities, do occur. Although, several studies have been conducted to assess, quantify and monitor water quality, soils and other natural resources in Calabar (Nganje et al. 2007; Edet et al. 2014), there exists no report of integrated pollution studies. Additionally, the few soil quality studies (e.g. Edet et al. 2014) are regional, and therefore, findings might have been wrongly generalised. Thus, information on the spatial distribution of physical properties of the vadose zone materials (VZM), lateral and vertical extents of soil and/or groundwater contaminated zones, which are necessary for broader assessment of contaminant distribution (Kaya et al. 2007), is presently unavailable. This study is aimed at employing integrated geophysical, geological and

geochemical data in examining the contamination levels of soil and water resources in Calabar, Nigeria.

## Physiography, location and geology of study area

### Location

Calabar is located between Latitudes 4°15' and 5°05'N of the Equator and Longitudes 8°10' and 8°30'E of the Greenwich Meridian, in Cross River State, southeastern Nigeria (Fig. 1a, b). With an areal extent of ~ 200 km<sup>2</sup>, Calabar is sited in the low-lying parts of the freshwater mangrove swamp forest of West Africa (Iloje 2001). Surface elevations in Calabar vary from < 1 m in the south to > 70 m in the north (Fig. 1b, c).

Calabar is located in a humid tropical climatic environment characterised by two seasons—wet and dry. The wet season, which usually begins in March and ends diffusely in October, corresponds to a period when the northward heading and moisture-laden Trans-Atlantic air mass, crosses the area. The peak of the rainy season conforms to a period with the highest static water levels (SWLs). Surface run-offs, resulting from heavy rains, usually dissolve, dislodge, transport and deposit some weakly cementing materials from the sand-dominated soils in the coastal areas and drainage channels, thereby leaving the epithelial sediments in a perpetually dry and sandy state. Dry season normally begins obliquely with a gradual increase in aridity and rising temperature in November and gradually eases out as April approaches. The beginning of dry season often marks the arrival of the southward heading Sahara Desert-borne Tropical continental air mass. Climatic data available at the Nigerian Meteorological Agency, Calabar and Department of Geography and Environmental Science, University of Calabar, Calabar show that between 1951 and 2015, variations in mean monthly temperature [minimum (*A*) and maximum (*B*)], rainfall (*C*) and relative humidity (*D*) are as shown in Fig. 2a–d, respectively.

### Location and generalised geology of Calabar

Calabar is located in a geologic environment that is dominated by Tertiary-Quaternary Coastal Plain Sands, CPSs (or Benin Formation) and Alluvial sediments. Cretaceous sediments of the Calabar Flank and rocks of Precambrian Oban Massif underlie these CPSs, which cover over 80% of the study area. Varying thicknesses of interfingering units of lacustrine, fluvial, loose and poorly sorted sands, pebbles, clays and lignite streaks are prevalent in the CPS. The alluvial units, which comprise tidal and lagoonal sediments, beach sands and soils, are more common in riverbanks,

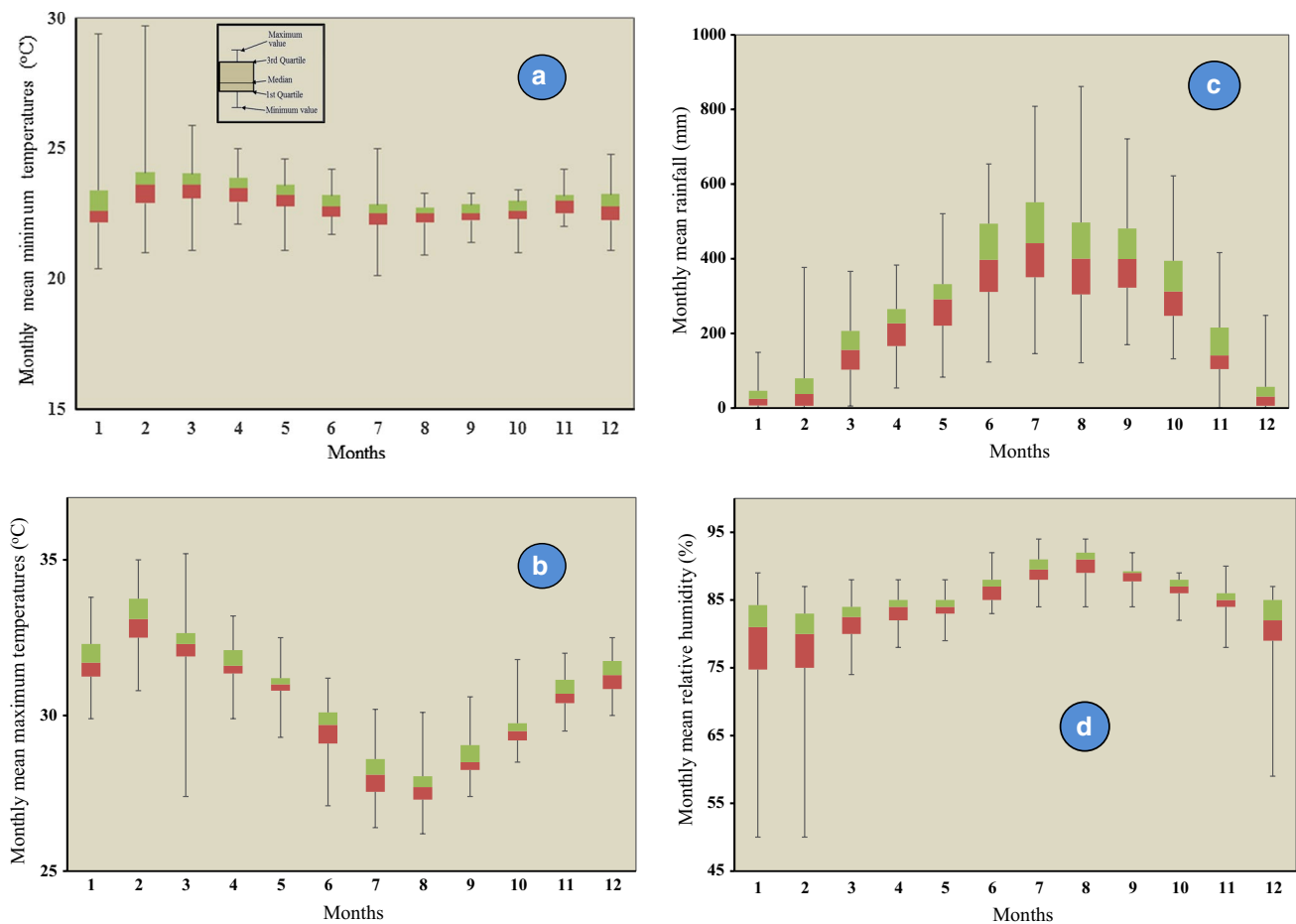


**Fig. 2** Box plots showing the distribution of monthly mean minimum (a) and maximum (b) temperatures, monthly mean rainfall (c) and relative humidity (d) in Calabar between 1951 and 2012

swamps and floodplains in the south (Reijers et al. 1987; Reijers and Petters 1987).

Alternating units of thin clays and lignite streaks truncate the vertical continuity of the CPSs aquifers, thus transforming them into multi-storey aquifer systems (Edet and Okereke 2002; Edet and Worden 2009). Lateritic sediments, with varying thicknesses, overlie the CPS aquifers in many locations. However, they are overtly exposed near the beaches and shorelines. Typical variations in SWLs are from < 1 to ~ 35 m in southern and northern areas, respectively. Geotechnical characterisation of the vadoze zone materials reveals the abundance of predominantly non-plastic sandy clay (permeability ranges from  $6.80 \times 10^{-3}$  to  $9.43 \times 10^{-3}$  cm/s) and gravelly clay with permeability variations of  $7.00 \times 10^{-1}$ – $8.70 \times 10^{-1}$  cm/s, sediments (Youde-wei and Nwankwoala 2010).

## Hydrogeology

Calabar is endowed with enormous water resources—rain, SWR and groundwater. Three southward flowing rivers:

Calabar River in the west, easterly Great Qua River and Cross River Estuary in the south (Fig. 1b, c), and a dense network of streams, which discharge into the rivers, are the main SWR that dominate the landscape of Calabar. The rivers and streams are part of the Cross River system that traverses both mangrove and freshwater swamps. The overall discharge of the Cross River varies from ~ 879 to ~ 2533 m<sup>3</sup>/s in dry and wet seasons, respectively (Lowenberg and Kunzel 1991).

Currently, households and industries operating in Calabar, contrary to the dominant practices few years ago, depend mainly on groundwater resource for all their water needs. Water quality studies conducted by Edet and Okereke (2002) and Edet and Worden (2009) reveal that the groundwater, commonly extracted from shallow water wells and boreholes (hand pumped and motorised), is potable. However, the upper part of the saturated aquifer is prone to microbial contamination in many locations (Akpan et al. 2002).

## Materials and methods

### Vertical electrical sounding data acquisition

Electrical resistivity (ER) method, a geophysical technique commonly used for economical mapping of subsurface materials based on resistivity contrasts between various lithologic units, was used. Relevant literatures are replete with reports of its successful applications, particularly in small-scale environmental investigations (Barte et al. 2010; Okoyeh et al. 2013). Consequently, two ER field procedures comprising vertical electrical sounding, VES and electrical resistivity tomography, ERT, were adopted in investigating the levels of soil and groundwater contamination in Calabar. A SSP-ATS-MRP model of IGIS resistivity meter was used for VES data acquisition because of its ability to measure very low ( $\sim 1 \mu\Omega$ ) resistances. VES data were acquired randomly at 60 sites (Fig. 1a) using Schlumberger electrode array between January 2012 and December 2015. Twenty sites were re-occupied in dry season to check for seasonal variations. The Schlumberger array was chosen because it can map vertical resistivity variations at both shallow and deeper depths (Al-Tarazi et al. 2006; Pánek et al. 2010).

Apparent resistivity curves obtained were smoothed and where necessary, outliers and other noisy segments arising from lateral changes in resistivity were cautiously removed. Trends and anomalous segments were identified by manually correlating the smoothed curves across neighbouring stations. Discontinuities in the smoothed curves were attributed to either changes in lithology or contamination. Apparent resistivities observed at  $AB = 4, 10, 20, 30$  and  $60$  m were contoured and stacked to obtain the pseudo-three-dimensional (3-D) resistivity variation pattern shown in Fig. 3.

The technique of partial curve matching of field and theoretical curves was used in obtaining preliminary layer parameters (PLP) (Orellana and Mooney 1966). The PLPs and smoothed data were used as inputs into the inversion stage that was performed using RESIST and WinRESIST codes (Vender Velpen 1988). The codes performed some mathematical calculations with the PLPs and generate some theoretical data, which they used the root mean square (RMS) technique in rating their matching levels with field data, in the process. Lithological data from nearby boreholes were used to constrain the interpreted results and where necessary, they were modified to obtain more suited geoelectric interpretation and also, determine the most appropriate resistivity values for the various lithological units. Samples of the modelled curves and their extents of correlation with geological models are shown in Fig. 4. However, in some locations ( $< 2\%$ ), particularly

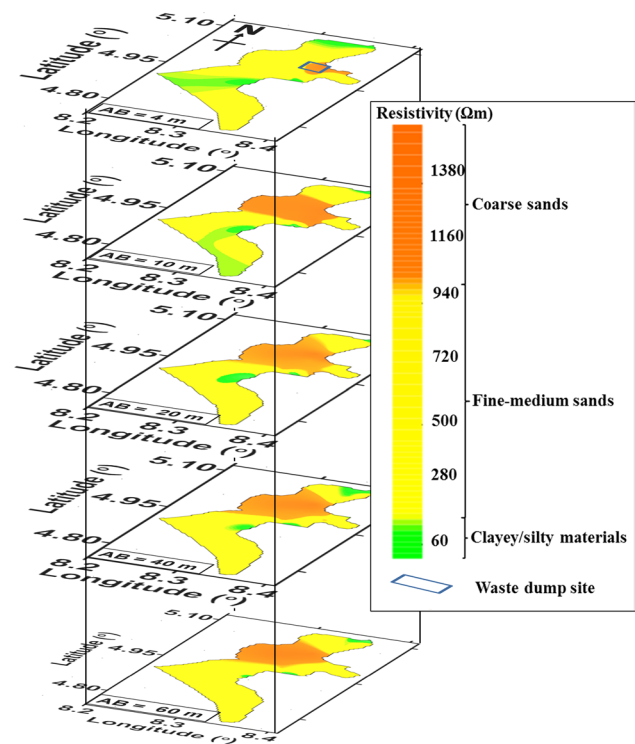
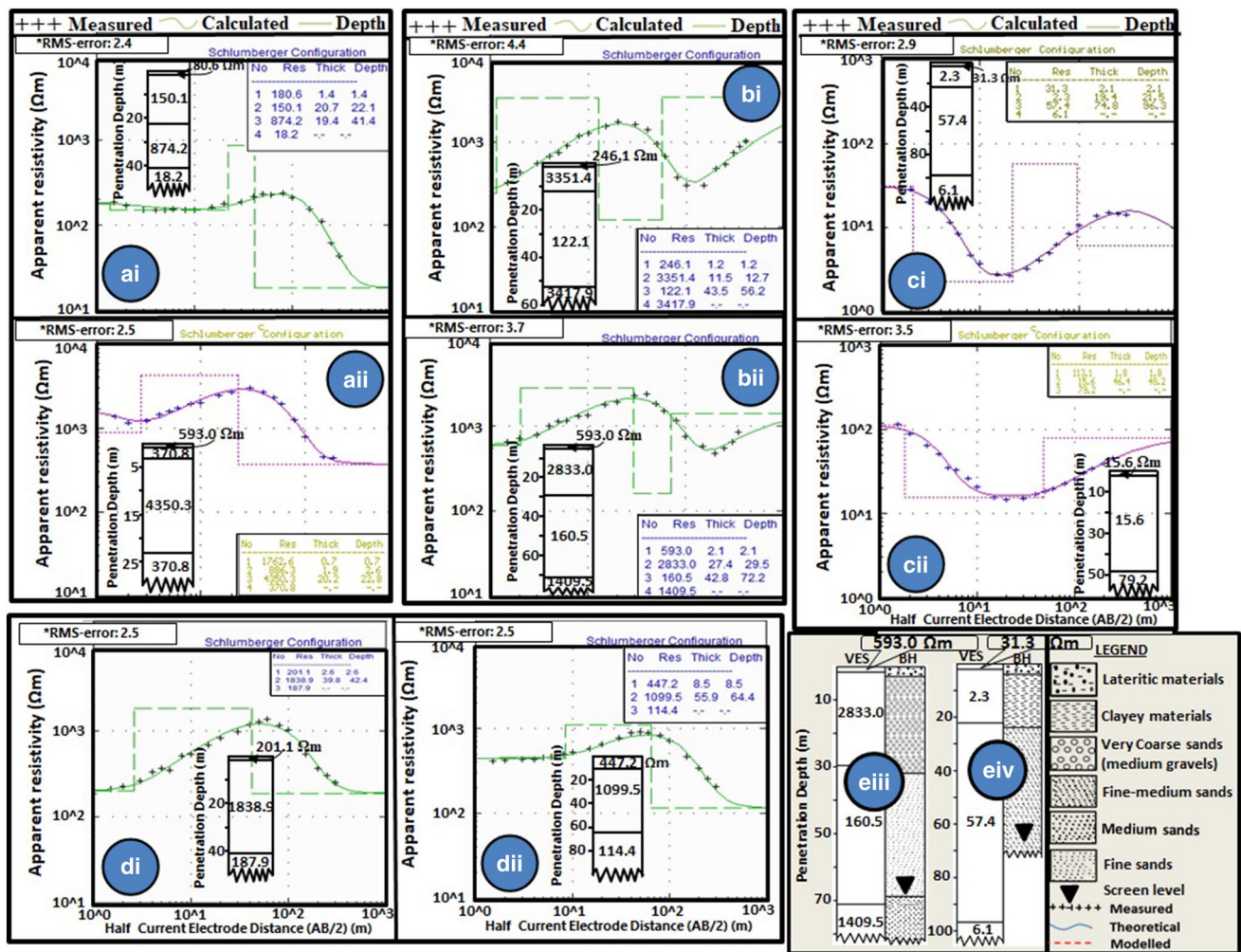


Fig. 3 Pseudo 3-D shallow surface resistivity distribution in Calabar

at the WDS, achieving satisfactory correlation was difficult and this problem was attributed to many factors like the presence of thin layer surrounded by thicker lithologic units, variations in the amount and quality of moisture contents of a layer and so on (Yadav et al. 2010). In addition, where the curves were originally distorted (Fig. 5), satisfactory modelling was difficult. Geological interpretation was performed by calibrating the layer parameters with lithological logs (Fig. 4e).

### Electrical resistivity tomography data acquisition

The electrical resistivity tomography (ERT) technique, a comparatively recent ER prospecting procedure, is commonly used for high-resolution electrostratigraphic modelling of complicated geological terrain. It has also been successfully used in modelling environments plagued by volcanic and geothermal (Revil et al. 2010; Hermans et al. 2012), landslide, rockslide and subsidence (Heincke et al. 2010; Rosales et al. 2012; Abidin et al. 2017) and seismotectonics (Caputo et al. 2003; Giocoli et al. 2013) disturbances. Furthermore, reports of its satisfactory applications in lithological mapping and characterisation (Casas et al. 2008; Sudha et al. 2009); hydrological monitoring (Giocoli et al. 2013; Wallin et al. 2013); soil and groundwater contamination (Halihan et al. 2012; Rao et al. 2014); environmental and engineering investigations (Akpan et al. 2009; Rosales



**Fig. 4** Samples of the dominant curve types—HK (**ai** and **aii**), KH (**bi** and **bii**), H (**ci** and **cii**) and K (**di** and **dii**) observed in Calabar, Nigeria. Correlation between VES and borehole lithologic logs at **bii** and **cii**. Insert: layer parameters and their corresponding 1-D resistivity model

et al. 2012; Meziani et al. 2017); and mapping of subsurface cavities and economic minerals (Mitrofan et al. 2007; Akpan et al. 2014a, b) exist. These reports of its optimal applications in environmental mapping influenced its choice in this study. In Calabar, high-voltage–power transmission and distribution lines, which can induce spurious signals, pass overhead in many locations of interest. Consequently, to suppress the effects of such signals on data quality, the Wenner electrode array, reputed for its capacity to generate data with high signal–noise ratio (Zhou et al. 2002; Loke 2004), was adopted in data acquisition. Besides, the Wenner array can optimally map vertical changes in resistivity although its capacity to discriminate horizontal discontinuities may not be very satisfactory (Zhou et al. 2002; Smith and Sjogren 2006).

The electrical resistivity tomography, ERT, investigations were conducted along four planar profiles to minimise topographic effects. Outside the WDS, the other ERT profiles

were randomly sited with minimum electrode spacing of 5 m and maximum spacing that vary according to profile length. Electrical contacts between the ground and electrodes were confirmed to be within the range necessary for optimal transmission of signals (160–230 Ωm) (Wilkinson et al. 2010). The reciprocal error (RPE) technique (Eq. 1), which 5% was fixed as maximum acceptable limit, was adopted for in situ data quality assessment.

$$RPE = 100 \frac{|\rho_f - \rho_r|}{\rho_f + \rho_r} \% \tag{1}$$

where  $\rho_f$  and  $\rho_r$  are the forward and reverse resistivities, respectively.

The RES2DINV code (Loke and Barker 1996), which, using smoothness–constrained least-squares inversion of pseudo-data, can produce two-dimensional (2-D) resistivity–depth model, was used in data modelling. The software

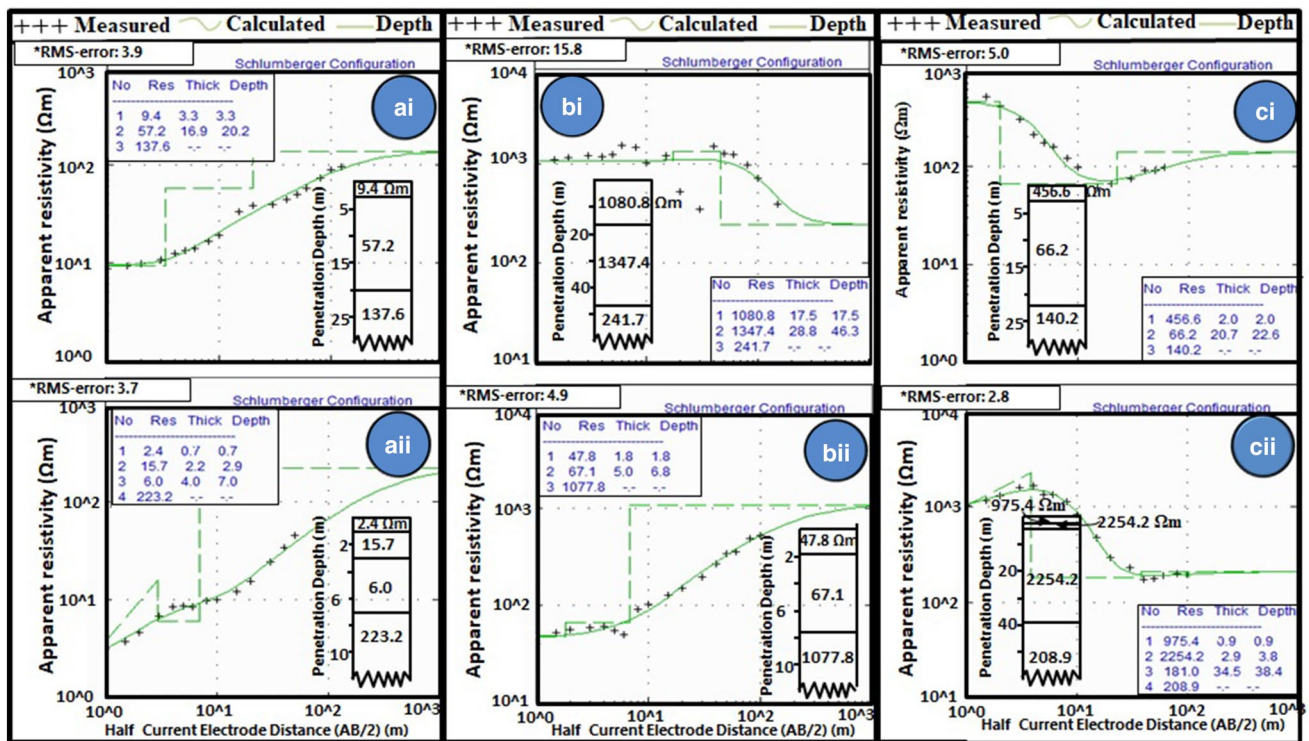


Fig. 5 Distorted VES curves obtained at the WDS. Insert: layer parameters and their corresponding 1-D model

subdivides the subsurface into uniform-resistivity rectangular blocks, equal in number to the total number of data points. It then uses the smoothness-constrained algorithm in generating models with smooth resistivity variations, compares the resistivities of each block with measured resistivities and finally, rate their differences using RMS technique. The RMS values were iteratively reduced (L1 norm) to acceptable levels. The number of numerical computations performed in the process was reduced using quasi-Newtonian optimisation scheme. Resistivities of observed models were interpreted by comparing them with standard resistivities of rocks (Telford et al. 1990). Subsurface images of the four ERT profiles are shown in Fig. 6. Lithological data were also used in calibrating ERT results.

### Soil and water sampling

#### Surface and groundwater sampling

Sampling of surface and groundwater resources was performed in two seasons with the aim of tracking seasonal variations. Dry season sampling was conducted between November, 2012 and March, 2015, while wet season sampling was performed between April, 2012 and October, 2015. Ten randomly distributed water samples, comprising five surface and five groundwater, were collected in pre-cleaned 1-L plastic bottles. The cleaning was done with distil

water and latter, with the water resource to be sampled three times. The groundwater samples were collected from boreholes, which in Calabar, are screened between 50 (south) and > 70 m (north). Two sets of SWR samples were collected by immersing the pre-cleaned polythene bottles inside the water bodies at Marina Beach along the Calabar River (1), Esuk Atu Beach along the Qua River (2), Adiabo Beach along the northern part of Calabar River (3), Edim Otop Stream (4) and leachate sample (5) from the WDS (Fig. 1b). The leachate samples were collected at the downstream part of the WDS so that their chemical signatures can be reasonably captured (Meju 2000). The samples were tightly corked. In situ measurements of some physico-chemical parameters: pH, total dissolved solids (TDS), electrical conductivity (EC) and temperature, were made using Combo EC and pH meter (Hanna HI98130) from Hanna Instruments, USA. The samples were cocked and stored in a refrigerator at 4 °C and latter transported to the laboratory for analyses. Suspended particles in the water samples were filtered out using 0.45-mm Millipore membrane papers.

The samples were analysed using spectrophotometric (Wagtech 7100 model) technique at the Cross River State Rural Water and Sanitation Agency (CR-RUWATSAN) Laboratory, Calabar. Standard procedures, like rinsing the cells with deionised water and shaking the samples before pouring 10 ml of each sample into them, specified in the American Public Health Association, APHA (2005)

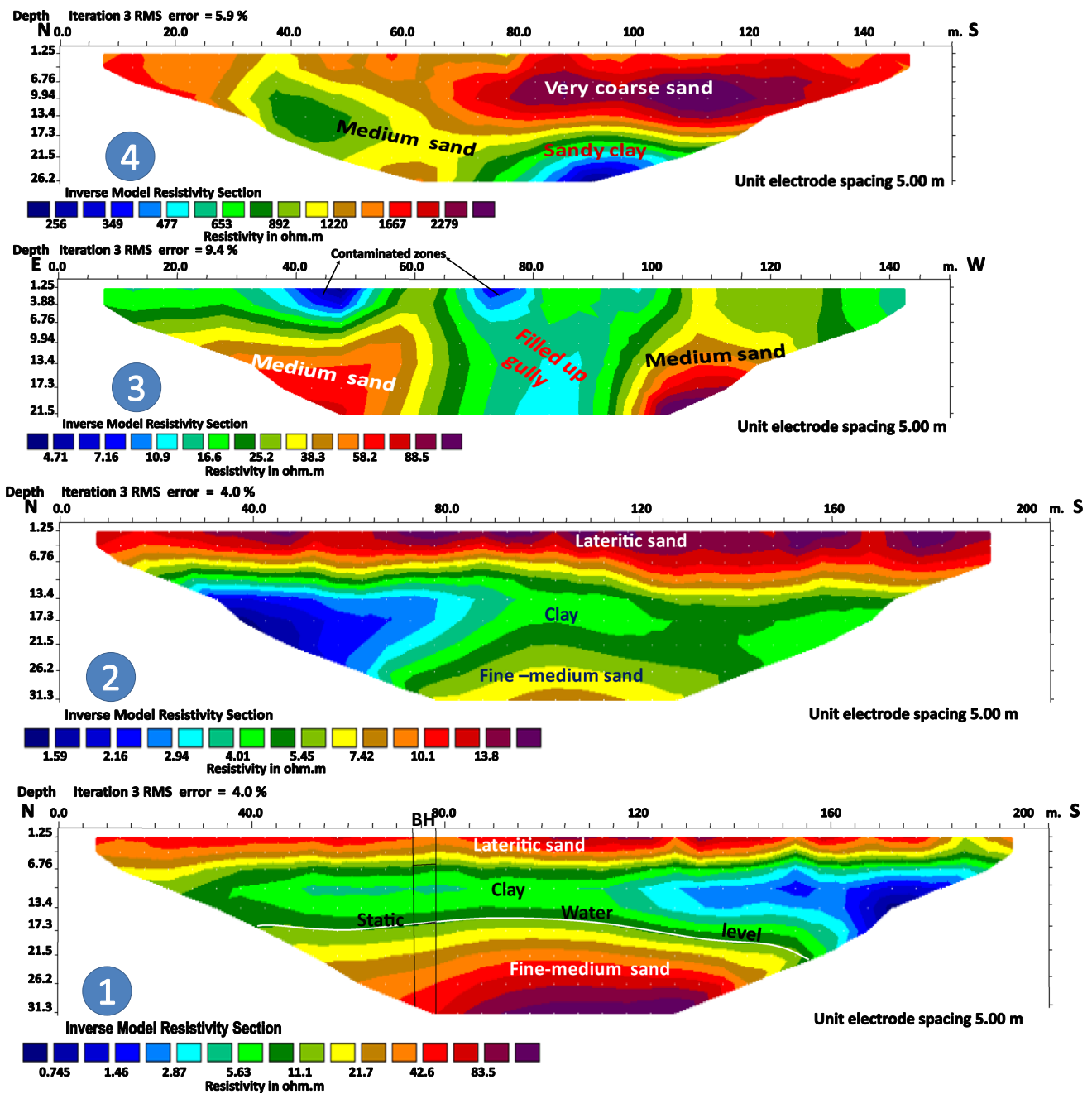


Fig. 6 2-D resistivity images obtained from the four profiles

were followed while conducting the analyses. All the analyses were performed with the aim of determining the concentrations of some cations: calcium ( $\text{Ca}^{2+}$ ), sodium ( $\text{Na}^+$ ), potassium ( $\text{K}^+$ ) and magnesium ( $\text{Mg}^{2+}$ ), and anions: nitrate ( $\text{NO}_3^-$ ), bicarbonate ( $\text{HCO}_3^-$ ), sulphate ( $\text{SO}_4^{2-}$ ) and chloride ( $\text{Cl}^-$ ). Measures adopted to obtain good data quality include analyses of blanks and duplicate samples and ion-balance ratio, which 10% was fixed as maximum tolerable limit.

### Soil sampling

Five randomly located but fairly distributed composite soil samples (~ 500 g), including a leachate-saturated soil, were collected from the upper 30-cm soil layer using plastic spatula (Fig. 1b). Before collecting the samples, the upper 2-cm soil layer was removed. This depth was considered to be reasonable because most anthropogenic contaminants, biogenic materials and plant nutrients, according to Krishna



and Govil (2007), usually settle within this depth range. The plastic scapular was always washed and dried before used in collecting fresh samples. The samples were stored in black-coloured double polythene bags before they were transported to the Soil Science Lab., University of Calabar, Nigeria for analyses.

The samples were air-dried and kept in oven for 48 h at 60 °C, crushed in a mortar and disaggregated into component parts by a 2-mm sieve. pH and EC of the soils were measured in soil/water suspension (1:1 ratio) using Combo EC and pH meter. Grain size analyses were performed using a 2-mm sieve in order to quantitatively rate their physical characteristics.

ISO 11277 (1998) guidelines were used in performing fluid extraction from the samples. The extracts were digested with a mixture of nitric and perchloric acids. The AAS technique was also used in determining their ionic concentrations. Results obtained from analyses of duplicate samples were used as control.

## Data analyses, results and discussion

### Hydrochemical results

Summary statistics of the main geochemical composition of SWR, groundwater and leachates is shown in Table 1. The anomalous properties of the leachates caused wide ranges in the results. SWR temperatures vary from 26.8 to 27.2 °C in wet, and 28.0 to 28.5 °C in dry seasons. Corresponding groundwater temperatures range from 29.6 to 30.2 and 28.6 to 28.9 °C, respectively. Excepting the leachates, where mean temperatures are 28.0 °C (wet) and 29.7 °C (dry), the water temperatures are within ranges reported in Edet et al. (2003), thus affirming the absence of significant changes in the conditions of the water bodies. In addition, the pattern of SWR temperature variations is in conformity to ambient temperatures although the mean groundwater temperature in rainy season is comparatively higher. In wet seasons, ambient temperatures are usually low and groundwater, characterised by comparatively higher heat capacity, absorbs and stores thermal energy. However, in dry season, the various SWR resources are uniformly heated by direct solar radiation and therefore, their temperatures are higher (Réveillère et al. 2013). The elevated temperature of leachates in wet season was attributed to increased rate of biochemically controlled exothermic reactions occurring inside them (MacFarlane et al. 1983).

Wet season pH observations for SWR are lower (4.50–5.81, mean of 5.32) than their dry season counterparts (6.20–6.80, mean of 6.50). Corresponding seasonal pH variations in groundwater are 6.10–6.30 (mean of 6.18) and 6.4–6.50 (mean of 6.44). Hence, both SWR and

groundwater exist under weakly acidic–neutral conditions. Increased concentrations of residual ions in dehydrating water bodies and discharge of carbonated (CO<sub>2</sub>-enriched) groundwater into SWR in dry season perhaps contributed to their marginal increase (Edet and Worden 2009). In wet seasons, discharge of organic matter-laden surface run-off into SWR bodies probably contributed to their acidic nature. Additionally, continuous falling of low acidic rain and possibly heavy leaching of chemical fertilizers into the aquifer horizons, especially in the south where the CPSs aquifers are exposed, might have contributed to their low acidic status (Scott et al. 2004; Srinivasamoorthy et al. 2014). Thus, apart from leachates, where wet and dry season pH observations are 6.60 and 7.50, respectively, and groundwater at some locations, water pH observations are generally slightly below the World Health Organisation, WHO (2004) recommended standard (6.5–8.5) for domestic and agricultural needs.

EC variations in SWR are 64.70–147.20 µS/cm (mean of 87.35 µS/cm) and 82.40–175.00 µS/cm (mean of 110.10 µS/cm) in wet and dry seasons, respectively. Their equivalent variations in groundwater are 227.10–242.50 µS/cm (mean of 236.90 µS/cm) and 174.5–188.50 µS/cm (mean of 180.34 µS/cm), respectively. The low ECs in SWR indicate their suitability for irrigation and drinking needs. However, the leachates (characterised by high ECs-7420.00 in wet and 8600.00 in dry seasons) are likely to harm the environment. The wide range in EC observations is reflective of variations in the amount of materials transported by the various SWR bodies across seasons. Groundwater is characterised by relatively stable ECs (mean range of 15.40 µS/cm) in dry season although wet season observations are slightly higher. In SWR, TDS varies from 48.20 to 117.40 mg/L (mean of 67.33 mg/L) in wet and 60.10 to 124.80 mg/L (mean of 77.85 mg/L) in dry seasons. Corresponding seasonal variations in groundwater are 119.20–199.90 mg/L (mean of 154.30 mg/L) and 97.20–142.50 mg/L (mean of 114.90 mg/L). Since Singh and Karra (1975) and Van Niekerk et al. (2014) have shown that TDS and EC are empirically related (Eq. 2), it implies that same factors are responsible for their enrichments.

$$\text{TDS} = \text{constant} \times \text{EC} \quad (2)$$

The constant, according to Metcalf & Eddy et al. (2003), varies between 0.55 and 0.70 with an average of 0.64.

Anionic species profusion levels in SWR are NO<sub>3</sub><sup>-</sup> (1%), HCO<sub>3</sub><sup>-</sup> (5%), SO<sub>4</sub><sup>2-</sup> (11%) and Cl<sup>-</sup> (84%); and Ca<sup>2+</sup> (2%), Mg<sup>2+</sup> (1%), K<sup>+</sup> (1%) and Na<sup>+</sup> (92%) for cations. Anionic abundances in groundwater are NO<sub>3</sub><sup>-</sup> (0%), SO<sub>4</sub><sup>2-</sup> (17%), Cl<sup>-</sup> (20%) and HCO<sub>3</sub><sup>-</sup> (62%) while the level of cationic enrichments are Mg<sup>2+</sup> (2%), K<sup>+</sup> (7%), Ca<sup>2+</sup> (7%) and Na<sup>+</sup> (84%). Mean ionic abundances in SWR for the two seasons are NO<sub>3</sub><sup>-</sup> (1%), SO<sub>4</sub><sup>2-</sup> (6%), HCO<sub>3</sub><sup>-</sup> (3%), Cl<sup>-</sup> (56%), Ca<sup>2+</sup> (1%), K<sup>+</sup> (1%), Mg<sup>2+</sup> (2%) and Na<sup>+</sup> (31%). Corresponding

**Table 1** Summary statistics of physico-chemical parameters of water in Calabar

Parameters/units	Season	Surface water								
		Minimum	Maximum	Range	Mean	% Abundance	Median	Standard deviation	Previous observations by Edet et al. (2003)	
Temperature (°C)	Wet	26.80	28.00	1.20	27.18		27.10	0.49		
	Dry	28.00	29.70	1.70	28.54		28.40	0.68	26.3–27.9	
	Mean	27.40	28.85	1.45	27.86		27.65	0.57		
pH	Wet	4.50	6.60	2.10	5.58		5.66	0.76		
	Dry	6.20	7.50	1.30	6.70		6.60	0.50	4.0–6.0	
	Mean	5.65	7.05	1.40	6.14		6.01	0.54		
EC (nS/cm)	Wet	64.70	7420.00	7355.30	1553.88		69.20	3279.44		
	Dry	82.40	8600.00	8517.60	1808.08		93.00	3796.99	41–264	
	Mean	75.35	8010.00	7934.65	1680.98		81.10	3538.21		
TDS (mg/L)	Wet	48.20	5110.00	5061.80	1075.86		52.40	2255.34		
	Dry	60.10	5900.00	5839.90	1242.28		64.00	2603.89	18.43–7934.72 <sup>a</sup>	
	Mean	55.70	5505.00	5449.30	1159.07		57.45	2429.61		
NO <sub>3</sub> (mg/L)	Wet	2.20	3.10	0.90	2.72	0.61	2.20	2.20		
	Dry	1.95	2.80	0.85	2.23	0.50	1.95	1.95	0–51.85	
	Mean	2.15	2.95	0.80	2.48	0.56	2.35	0.34		
HCO <sub>3</sub> (mg/L)	Wet	12.30	52.40	40.10	21.12	4.76	13.70	17.50		
	Dry	10.80	32.10	21.30	15.72	3.50	12.30	9.19	7.32–138.00	
	Mean	11.65	42.25	30.60	18.42	4.13	13.00	13.34		
SO <sub>4</sub> (mg/L)	Wet	14.20	19.80	5.60	18.22	4.10	19.20	2.35		
	Dry	15.00	42.40	27.40	32.32	7.19	40.60	12.80	0.00–834.21	
	Mean	14.60	31.10	16.50	25.27	5.65	30.20	7.48		
Cl <sup>-</sup> (mg/L)	Wet	232.70	330.00	97.30	258.68	58.25	243.50	40.40		
	Dry	213.61	340.00	126.39	248.64	55.29	231.20	51.60	0.00–4368.17	
	Mean	223.16	335.00	111.85	253.66	56.77	234.95	45.92		
Ca <sup>2+</sup> (mg/L)	Wet	2.20	4.60	2.40	2.78	0.63	2.40	1.02		
	Dry	3.00	4.10	1.10	3.28	0.73	3.10	0.47	0.00–81.36	
	Mean	2.60	4.35	1.75	3.03	0.68	2.70	0.74		
Na <sup>+</sup> (mg/L)	Wet	123.30	155.70	32.40	133.00	29.95	125.90	13.84		
	Dry	130.00	170.40	40.40	139.26	30.97	131.20	17.45	2.82–2814.41	
	Mean	126.70	163.05	36.35	136.13	30.46	128.55	15.42		
K <sup>+</sup> (mg/L)	Wet	3.50	6.10	2.60	4.34	0.98	4.10	1.02		
	Dry	4.30	5.30	1.00	4.78	1.06	4.80	0.36	0.24–81.31	
	Mean	4.05	5.70	1.65	4.56	1.02	4.40	0.66		
Mg <sup>2+</sup> (mg/L)	Wet	2.80	4.30	1.50	3.26	0.73	3.10	0.60		
	Dry	3.00	3.80	0.80	3.50	0.78	3.70	0.34	0.01–193.93	
	Mean	2.95	4.05	1.10	3.38	0.76	3.40	0.43		
Parameters/units	Season	Groundwater								
		Minimum	Maximum	Range	Mean	% Abundance	Median	Standard deviation	Previous observations by Edet et al. (2003)	WHO (2004)
Temperature (°C)	Wet	29.60	30.20	0.60	29.96		30.00	0.23		
	Dry	28.60	28.90	0.30	28.76		28.80	0.11	26–29.7	Ambient
	Mean	29.20	29.45	0.25	29.36		29.45	0.12		
pH	Wet	6.10	6.30	0.20	6.18		6.20	0.08		
	Dry	6.40	6.50	0.10	6.44		6.40	0.05	3.3–5.3	6.5–8.5
	Mean	6.25	6.40	0.15	6.31		6.30	0.05		

**Table 1** (continued)

Parameters/units	Season	Groundwater								
		Minimum	Maximum	Range	Mean	% Abundance	Median	Standard deviation	Previous observations by Edet et al. (2003)	WHO (2004)
EC (nS/cm)	Wet	227.10	242.50	15.40	236.90		236.90	6.28		
	Dry	174.50	188.50	14.00	180.34		177.10	6.52	35–352	1500
	Mean	206.40	211.55	5.15	208.62		208.40	1.89		
TDS (mg/L)	Wet	119.20	199.90	80.70	154.30		151.70	29.27		
	Dry	97.20	142.50	45.30	114.90		111.80	18.08	13.3–291.29 <sup>a</sup>	1000
	Mean	115.50	148.55	33.05	134.60		132.80	13.69		
NO <sub>3</sub> (mg/L)	Wet	0.12	0.19	0.07	0.16	0.15	0.18	0.03		
	Dry	0.27	0.50	0.23	0.37	0.42	0.37	0.09	0.00–87.49	50
	Mean	0.21	0.31	0.10	0.27	0.29	0.28	0.04		
HCO <sub>3</sub> (mg/L)	Wet	45.40	49.20	3.80	47.18	42.98	47.50	1.73		
	Dry	42.60	43.40	0.80	42.94	48.46	42.90	0.30	4.92–117.60	300
	Mean	44.00	46.30	2.30	45.06	45.72	45.20	0.96		
SO <sub>4</sub> (mg/L)	Wet	5.20	8.30	3.10	7.11	6.48	7.70	1.38		
	Dry	13.60	17.90	4.30	15.84	17.87	15.70	1.59	0.00–47.47	250
	Mean	9.87	12.80	2.94	11.48	12.18	12.00	1.31		
Cl <sup>-</sup> (mg/L)	Wet	11.40	18.84	7.44	16.35	14.89	17.10	2.93		
	Dry	9.50	10.60	1.10	9.96	11.24	9.80	0.44	0.00–42.22	250
	Mean	10.45	14.72	4.27	13.15	13.07	13.65	1.63		
Ca <sup>2+</sup> (mg/L)	Wet	2.18	2.50	0.32	2.36	2.15	2.40	0.16		
	Dry	1.36	1.60	0.24	1.49	1.68	1.50	0.11	0.01–16.15	200
	Mean	1.80	2.05	0.25	1.92	1.92	1.88	0.12		
Na <sup>+</sup> (mg/L)	Wet	32.10	35.20	3.10	33.68	30.68	33.80	1.37		
	Dry	14.80	16.20	1.40	15.64	17.65	15.80	0.53	2.15–50.54	200
	Mean	23.65	25.55	1.90	24.66	24.17	24.80	0.76		
K <sup>+</sup> (mg/L)	Wet	2.40	2.50	0.10	2.46	2.24	2.50	0.05		
	Dry	1.40	2.00	0.60	1.78	2.01	1.80	0.23	0.24–7.75	30
	Mean	1.95	2.25	0.30	2.12	2.13	2.10	0.12		
Mg <sup>2+</sup> (mg/L)	Wet	0.40	0.50	0.10	0.46	0.42	0.50	0.05		
	Dry	0.56	0.62	0.06	0.59	0.67	0.60	0.02	0.01–2.11	150
	Mean	0.49	0.55	0.07	0.53	0.55	0.53	0.03		

<sup>a</sup>From Edet and Worden (2009)

variations in groundwater are NO<sub>3</sub><sup>-</sup> (0%), SO<sub>4</sub><sup>2-</sup> (12%), Cl<sup>-</sup> (13%) and HCO<sub>3</sub><sup>-</sup> (45%) for anions, Mg<sup>2+</sup> (2%), Ca<sup>2+</sup> and K<sup>+</sup> (2%) and Na<sup>+</sup> (25%). Thus, Na<sup>+</sup> and Cl<sup>-</sup> account for 88% of total ionic abundance in SWR, while Na<sup>+</sup> and HCO<sub>3</sub><sup>-</sup> dominate (70%) ionic loading in groundwater.

Nitrate concentrations in SWR vary from 2.20 to 3.10 mg/L (mean of 2.72 mg/L) and 1.95–2.80 mg/L (mean of 2.23 mg/L) in wet and dry seasons, respectively. In groundwater, it ranges from 0.12 to 0.19 mg/L (mean of 0.16 mg/L) in wet, and 0.27 to 0.50 mg/L (mean of 0.37 mg/L) in dry seasons. These results are < 50 mg/L concentration limit fixed by WHO (2004) for drinking and agricultural water needs. Furthermore, it is also within the

0.00–87.49 mg/L concentration levels reported by Edet et al. (2003) for water resources in the area. Nitrate concentration in water, although usually influenced by prevailing economic and industrial activities, is always low (< 3 mg/L) and if this arbitrary threshold is exceeded, then contamination, induced by anthropic sources, should be suspected (Eckhardt and Stackelberg 1995; Jalali 2010). Thus, the leachates with higher nitrate concentrations are contaminated. However, higher nitrate concentrations in drinking water, which, presently, is an issue of immense concern because of the dangers they pose to human and environmental healths (WHO 2004), have been reported in Calabar and even elsewhere (e.g. Gillis and Birch 2006; Edet and Worden 2009; Jalali 2010). Agricultural practices

such as indiscriminate application of nitrogenous fertilizers (e.g. urea and NPK), and dumping of human wastes, especially at the WDS, where higher concentrations exist, are probable sources of its enrichments. Improper management of organic manure and unsuitable operation and management of septic tanks could also be a contributor (Sujatha and Reddy 2003; Lee and Song 2007).

In SWR, wet and dry season variations in sulphate concentrations are 14.20–19.80 and 15.00–42.40 mg/L, respectively, while corresponding variations in groundwater are 5.20–8.30 and 13.60–17.90 mg/L. These observations, which are less than WHO (2004)'s maximum permissible limit of 250 mg/L, were attributed to natural pollution by pyritic substances that abound in the oxygen-enriched swamps. Additionally, their low concentrations across seasons might have been sustained by continuous breaking down of sulphates with higher concentration (Srinivasamoorthy et al. 2014). Singh (1994) identified other probable sources of sulphate enrichments, which are also prevalent in Calabar, to include leaching of fertilizers and municipal solid wastes, and dissolution of filtering water.

Bicarbonates, the most abundant ionic species in groundwater, are one of the primary buffering species that constitute alkalinity—a parameter commonly used for assessing the capacity of water to resist changes in its pH.  $\text{HCO}_3^-$  concentrations in groundwater vary from 45.40 to 49.20 mg/L (mean of 47.18 mg/L) and 44.00 to 46.30 mg/L (mean of 45.06 mg/L) during wet and dry seasons, respectively. In SWR, their concentrations range from 12.30 to 52.40 mg/L (mean of 21.12 mg/L) in wet, and 10.80 to 32.10 mg/L (mean of 15.72 mg/L) in dry seasons. These results are within WHO (2004) permissible limit of 300 mg/L. Many factors, including dissolution of carbonate minerals, e.g. calcite ( $\text{CaCO}_3$ ), dolomite ( $\text{CaMg}(\text{CO}_3)_2$ ) and aragonite, which are in high abundance in the adjoining Oban Massif and dissolution of atmospheric  $\text{CO}_2$  by rainwater and VZM, probably contributed to their enrichment (Rao 2002, 2006). However, at the WDS, carbonate-laden wastes and other decomposed organic materials, probably, contributed to its elevated abundance.

Chlorine occurs naturally in all water resources, and its concentration is a parameter commonly used for assessing their suitability for irrigation. At low concentrations, it supports the optimal growth of plants and animals.  $\text{Cl}^-$  concentrations in SWR are 213.61–340.00 mg/L (mean of 248.64 mg/L) and 232.70–330.00 mg/L (mean of 258.68 mg/L) in dry and wet seasons, respectively. In groundwater, 9.50–10.60 mg/L (mean of 9.96 mg/L) and 11.40–18.84 mg/L (mean of 16.35 mg/L) are their respective equivalent concentrations. These results are below the 250 mg/L permissible limit (WHO 2004). However, in the leachates, higher concentrations of  $\text{Cl}^-$  are prevalent.  $\text{Cl}^-$  enrichment in drinking water is probably caused by

many factors including tidal flushing-induced seawater intrusion especially in southern Calabar (Edet and Worden 2009), erosion and weathering of granitic rocks, e.g. hornblende and mica (Sujatha and Reddy 2003), that are prevalent in adjoining Oban Massif. Dominance of  $\text{Cl}^-$  over other anions in SWR in northern Calabar was attributed to fluids liberated by decomposed materials in the WDS (Pettyjohn 1971).

$\text{Na}^+$  concentrations (123.30–155.70 mg/L) in SWR in wet season, while sustaining their traditional affinity with  $\text{Cl}^-$  in the enrichment process, are marginally higher than their dry season (130.00–170.40 mg/L) profusion level. Concentration levels of other cations in SWR are 2.20–4.60 mg/L (mean of 2.40 mg/L) and 3.00–4.10 mg/L (mean of 2.40 mg/L) for  $\text{Ca}^{2+}$ ; 3.50–6.10 and 4.30–5.30 mg/L (mean of 4.78 mg/L) for  $\text{K}^+$ ; and 2.80–4.30 and 3.00–3.80 mg/L for  $\text{Mg}^{2+}$  in wet and dry seasons, respectively. Equivalent variational trends in groundwater are  $\text{Ca}^+$  (2.18–2.50 and 1.36–1.60 mg/L),  $\text{K}^+$  (2.40–2.50 and 1.40–2.00 mg/L) and  $\text{Mg}^{2+}$  (0.40–0.50 and 0.49–0.55 mg/L) (Table 1). Thus, cation profusion levels in SWR are higher than their groundwater counterparts. These cation abundances are all below WHO (2004) permissible limits of 200, 200, 30 and 150 mg/L for  $\text{Na}^+$ ,  $\text{Ca}^{2+}$ ,  $\text{K}^+$  and  $\text{Mg}^{2+}$ , respectively. Elevated concentrations of Na, Mg and Ca ions in water were attributed to cation exchange among minerals and perhaps, at the WDS, sewage contamination. Interaction of water with weathering products of some minerals, e.g. feldspars, pyroxenes, hornblendes and amphiboles and their accessories: albites, apatites and fluorites, which are in high abundance in the surrounding Oban Massif, probably, contributed to their enrichments (Edet and Worden 2009). In southern Calabar, seawater intrusion induced by tidal forces could perhaps be a minor contributor to the slight increase in  $\text{Na}^+$  and  $\text{Mg}^{2+}$  concentrations. Dissolution of clay, gravel, feldspar and, possibly, agricultural practices like undue application of inorganic fertilizers are likely to be other minor contributors (Kolachi and Jalali 2006; Srinivasamoorthy et al. 2008).

### Grain size distribution and soil chemistry results

Results of grain size analyses reveal the predominance of sediments with high sandy composition (78.4–91.2%) (Table 2). Geochemical compositions of the soils and their basic statistics are present in Fig. 7. Silty and alluvial sediments, which exist mainly in fluvial terraces, are of low profusion ( $\leq 8\%$ ). Clays are low–moderate in abundance (6.7% in leachate-saturated soils and 23.6% elsewhere). Thus, excepting the leachate-saturated soils, Calabar soils are nearly homogeneous in lithological composition. The low clay contents, particularly in the southern areas where the aquifers are overlain by very little or no protective materials, imply that the soils have low absorption capacities (Çolak 2012). But, in the northern parts, the aquifers are overlain

**Table 2** Results of physico-chemical and grain size analyses of soils in Calabar

S/no.	Name and position coordinates of sampling points														
	Location name	Sample code	Position coordinates of sampling point												
1	Jebbs street	S1	04°54'58.1"N	08°14'11.6"E											
2	Besides federal government girls	S2	04°59'09.9"N	08°21'18.5"E											
3	Satellite town	S3	04°57'29.4"N	08°21'17.9"E											
4	Akai efa swamp	S4	05°00'39.5"N	08°22'22.2"E											
5	Atimbo swamp	S5	04° 57'40.5"N	08°21'36.2"E											
6	Lenma road	S8	05°02'19.2"N	08°21'31.0"E											
7	Enima estate	S9	05°03'05.7"N	08°20'39.3"E											
8	Unical palm plantation	S10	04°57'28.7"N	08°21'10.0"E											
9	Waste dump 1	S6	05°02'01.0"N	08°21'51.4"E											
10	Waste dump 2	S7	05°02'00.8"N	08°21'51.4"E											
	Minimum														
	Maximum														
	Mean														
	Median														
	Range														
	Standard deviation														
	Control (Edet et al. 2014)														
	Pemissible Limit (Alloway 1990)														
	Threshold values (CCME 1999)														
	Average concentration in soils (FPDD 1990)														
S/no.	Measured parameters (mg/kg)											Particle size analyses (%)			
	pH	EC (uS/cm)	K <sup>+</sup>	Na <sup>+</sup>	NH <sup>4+</sup>	Ca <sup>2+</sup>	Mg <sup>2+</sup>	Al <sup>3+</sup>	Cl <sup>-</sup>	NO <sub>3</sub>	NO <sub>2</sub> <sup>-</sup>	SO <sub>4</sub>	Clay	Silt	Sand
1	5.0	35.0	0.10	0.08	4800	5.2	1.4	0.36	5.30	432.20	14.91	685.62	15.0	8.7	76.3
2	5.0	56.0	0.08	0.06	4480	4.0	1.3	0.40	5.86	338.26	20.45	457.08	11.0	9.7	79.3
3	4.7	62.0	0.08	0.07	4800	3.0	1.2	0.56	5.30	451.01	16.61	380.90	12.0	5.7	82.3
4	5.7	45.0	0.07	0.05	3520	5.2	1.8	0.24	5.96	281.88	15.76	304.72	13.0	9.7	77.3
5	5.6	66.2	0.06	0.06	3480	5.1	1.7	0.27	6.01	277.02	15.45	298.40	14.0	9.9	76.1
6	4.8	43.0	0.09	0.07	4450	4.0	1.4	0.66	5.89	338.05	18.32	304.72	15.0	7.7	77.3
7	4.9	42.2	0.10	0.60	4520	3.6	1.2	0.59	5.91	328.06	17.82	295.60	14.0	7.8	78.2
8	4.9	59.9	0.09	0.08	4640	3.6	1.1	0.47	5.30	440.10	16.20	390.10	11.6	11.1	77.3
9	7.6	916.0	0.13	0.09	5920	7.4	0.8	0.00	6.62	357.05	17.89	380.40	8.0	4.8	87.2
10	7.7	907.0	0.15	0.08	5050	7.2	0.9	0.00	6.59	369.11	17.56	383.00	7.0	4.7	88.3
	4.7	35.0	0.06	0.05	3480	3.0	1.1	0.00	5.30	277.02	14.91	295.60	11.0	5.7	76.1
	5.7	66.2	0.10	0.60	4800	5.2	1.8	0.66	6.01	451.01	20.45	685.62	15.0	11.1	82.3
	5.1	51.2	0.08	0.13	4336	4.2	1.4	0.44	5.69	360.82	16.94	389.64	13.2	8.8	78.0
	5.0	50.5	0.09	0.07	4500	4.0	1.4	0.44	5.87	338.15	16.41	342.81	13.5	9.2	77.3
	1.0	31.2	0.04	0.55	1320	2.2	0.7	0.66	0.71	173.99	5.54	390.02	4.0	5.4	6.2
	0.4	11.3	0.01	0.19	533	0.8	0.2	0.15	0.33	70.58	1.83	133.00	1.5	1.7	2.0
	5.3	19.0	6.04	13.60		22.8	21.8								
	4.0–8.5	4000	> 80												
	6.0–8.0														
	5.1–6.0	400	0.6–1.2	0.7–2.0	–	10.0–25.0	3.0–8.0								

by reasonably thick ( $\geq 10$  m) clayey/lateritic sediments with the argillaceous components increasing with depth, thereby enhancing their attenuating capacities (Meju 2000).

Undisturbed soils are slightly acidic (4.70–5.60) while the leachate-contaminated soils are characterised by slight alkalinity (pH > 7.0) although still within the 6.0–8.0

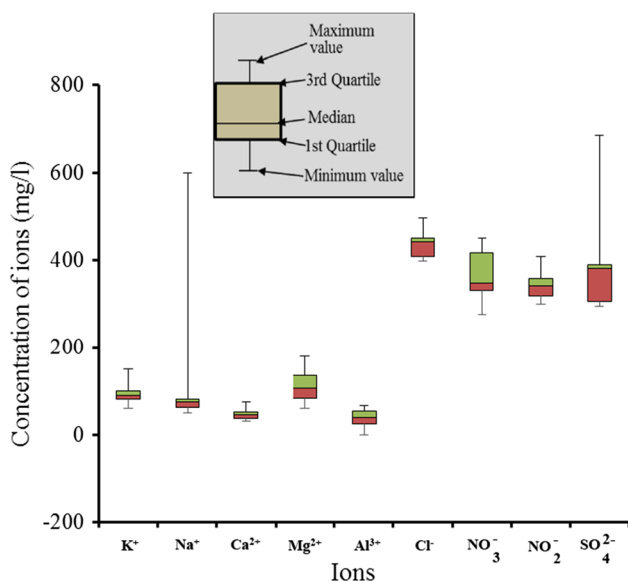


**Fig. 7** Box-Whisker plot showing the chemical constituents of soils in Calabar. (Concentrations of  $K^+$ ,  $Na^+$ ,  $Ca^{2+}$ ,  $Mg^{2+}$ ,  $Al^{3+}$ ,  $Cl^-$  and  $NO_2^-$  have been magnified by 1000, 1000, 10, 100, 100, 75, and 20, respectively, to enhance visual appreciation of the various boxes)

permissible range (Canadian Council of Ministers of the Environment, CCME 1999). These results correlate strongly with water pH observations. Since pH has logarithmic effects on soils, soils at the WDS, where high pH ( $> 7$ ) exist, are contaminated. Soil ECs, SEC (a measure of the amount of salts in soils), vary from 35.0 to 66.0  $\mu S/cm$  but at the WDS, SECs are higher ( $> 900 \mu S/cm$ ). Generally, all SECs are below the 4000  $\mu S/cm$  permissible limit (Alloway 1990). SEC, a parameter commonly used for assessing the state of soil health, shows that the soils are still appropriate for crop germination, growth and yield. It also reveals that plant nutrients are freely available with high activities of some soil microorganisms. Two factors comprising natural (e.g. soil mineral, climate and soil texture) and anthropogenic (e.g. type of cropping practice, irrigation, land use and extent of application of both organic like compost manure and inorganic fertilizers) affect their levels in the soils. The high SECs at the WDS were attributed to the influence of leachates originating from decomposing salt-enriched wastes. Metal ions present at the WDS might, probably, be a minor contributor to its slight elevation.

Soil cationic concentrations are 0.06–0.15 mg/kg for K, 0.05–0.60 mg/kg for Na, 3480–5920 mg/kg for  $NH_4$ , 3.00–7.40 mg/kg for Ca, 0.60–1.80 mg/kg for Mg and 0.00–0.66 mg/kg for  $Al^{3+}$ . Equivalent soil anionic concentrations are 5.30–6.62, 277.02–451.01, 14.91–20.45 and 295.60–685.62 mg/kg. Their mean concentrations, standard deviations and other basic statistics are shown in Table 2 and Fig. 7. In many cases, their ionic concentrations, though within tolerable limit (Table 2), are anomalous. The

high concentration of  $Cl^-$  in leachate-saturated soils might impede normal growth, photosynthetic capacity and yield of some plants (Dang et al. 2008).

## Electrical resistivity results

The one-dimensional (1-D) resistivity model reveals the presence of a 3–5-layered electrostratigraphic sequence with K-(50%) and KH-(25%) curves dominating stations with ABs below and above 600 m, respectively (Table 3). The epithelial sediments, characterised by low–moderately high resistivities ( $\sim 50 \Omega m$ ), are prevalent in undisturbed areas. However, at the swampy, WDS and the reclaimed areas, sampled layers are characterised by H and A curves and the capping sediments are characterised by low resistivities ( $\leq 30 \Omega m$ ).

Three-layer curve types exist mainly in the intact areas, and their distributions for low ABs ( $\leq 500$  m) are K (60%), KH (25%) and HK (15%). These results confirm the dominance of K-type (bell-shaped) curves reported by Edet and Okereke (2002). The epithelial sediments are characterised by low–moderately high resistivities (31.3–1973.5  $\Omega m$ ) and variable thicknesses ( $< 1$ –18 m). The resistivity variation pattern captures the changing lithologic and moisture compositions (lateritic clays, clayey/silty sands and fine–medium–coarse sands) of the capping sediments. Low resistivity sediments, observed mainly at locations where alluvial and cretaceous sediments abound, are prevalent in southern, southwestern and northern parts. Sediments with high resistivities occur extensively at locations where lateritic and gravelly clays exist (Fig. 3). Resistivity variations in the second layer, characterised by variable depths to bottom (4.0–64.1 m), range from  $\sim 2.2 \Omega m$  in the swampy terrain to 3588.6  $\Omega m$  in northcentral and western areas. The wide resistivity (6.0–1648.1  $\Omega m$ ) and depth to bottom (8.0–96.3 m) variations in the third layer are suspected to be caused by textural variabilities (silty/fine to medium–coarse sands) of the sediments. Where observed, resistivity variations in the fourth and fifth layers, characterised by variable depths to bottom (30.5–82.0 m), vary from 6.1 to 3417.9 and 70.0 to 180.0  $\Omega m$ , respectively. No significant seasonal changes in resistivity were observed except that first-layer resistivities reduce by factors of  $\sim 10$ –15% of their wet season values.

ERT results affirm the abundance of low–moderately high resistivity sediments in the shallow surface lithostratigraphic units. The thin ( $< 10$  m in ERTs 1 and 2, and  $\sim 18$  m in ERT 4) epithelial sediments are characterised by comparatively high resistivities: 20–80  $\Omega m$  (ERT 1),  $> 10 \Omega m$  (ERT 2) and  $> 1220 \Omega m$  (ERT 4). However, along ERT 3 (sited in a disturbed area), thinner ( $< 6$  m) and low resistivity ( $< 10 \Omega m$ ) sediments, attributed to leachate contamination, exist at horizontal distances of between 30–60 and 65–80 m

**Table 3** Summary of VES modelling results

S/no.	Curve type	Curve statistics	Maximum current electrode separation (m)	% Occurrence	Geoelectric layer resistivity ( $\Omega\text{m}$ )					Estimated depth to bottom			
					1	2	3	4	5	1	2	3	4
1	A	Minimum	400	3.3	9.4	57.2	137.6	–	–	1.8	6.8	–	–
		Maximum	500		47.8	67.1	1077.8	–	–	3.3	20.2	–	–
		Mean			28.6	62.2	607.7	–	–	2.6	13.5	–	–
2	H	Minimum	300	6.7	41.5	7.5	79.2	–	–	1.8	6.7	–	–
		Maximum	500		456.6	66.2	180.6	–	–	2.3	48.2	–	–
		Mean			203.7	29.8	133.3	–	–	2.0	25.8	–	–
3	HK	Minimum	250	20.0	31.3	2.2	38.1	6.1	–	1.3	12.6	41.4	–
		Maximum	800		511.2	2821.5	1375.7	106.2	–	2.1	23.6	96.3	–
		Mean			246.3	661.5	587.3	37.6	–	1.7	20.3	66.6	–
4	HKH	Minimum	600	5.0	180.6	110.0	208.7	18.2	70.0	1.2	5.0	8.0	30.5
		Maximum	600		268.4	709.4	662.6	74.9	81.8	2.0	22.1	41.4	80.5
		Mean			225.3	323.2	469.3	1582.8	83.3	1.3	12.9	24.7	60.1
5	KQ	Minimum	500	5.0	54.9	1214.1	227.1	60.0	–	0.6	6.1	16.3	–
		Maximum	500		499.7	6406.6	488.6	2303.5	–	2.4	19.2	50.7	–
		Mean			208.3	3675.6	1865.0	868.8	–	1.9	11.7	34.4	–
6	K	Minimum	200	30.0	50.3	392.7	119.5	–	–	1.0	16.1	–	–
		Maximum	600		1080.8	3588.6	241.7	–	–	18.0	64.1	–	–
		Mean			322.4	1596.5	181.8	–	–	5.0	46.1	–	–
7	KH	Minimum	300	25.0	2.4	14.7	6.0	149.5	–	1.0	4.0	8.0	–
		Maximum	900		975.4	3351.4	1482.4	3417.9	–	5.0	29.5	72.2	–
		Mean			257.6	1171.1	1588.6	897.3	–	1.3	9.5	35.4	–
8	KHK	Minimum	600	5.0	370.1	514.9	284.6	339.1	142.0	1.0	12.0	18.3	77.9
		Maximum	700		1973.5	1025.6	1648.1	619.8	180.0	5.0	26.0	60.2	82.0
		Mean			1171.8	770.3	966.4	479.5	162.0	2.8	14.4	36.2	80.0
	Minimum				2.4	2.2	6.0	6.1	70.0	0.6	4.0	8.0	30.5
	Maximum				1973.5	6406.6	1648.1	3417.9	180.0	18.0	64.1	96.3	82.0

along the profile. Resistivity variations between profiles were attributed to varying textural and moisture compositions of the sediments. Dominantly low resistivity sediments ( $< 20 \Omega\text{m}$  at ERT 1 and  $< 10 \Omega\text{m}$  at ERT 2), attributable to clays, clayey sands and lateritic materials, underlie the top layer. The argillaceous components are useful in reducing infiltration rate and, therefore, help in protecting the aquifers from contamination (Gemail et al. 2011) even though their efficiencies depend on their thicknesses and amount of contaminants. But in ERT 4, the capping high resistivity coarse sands are underlain by medium sands with comparably moderate resistivities.

Increase in resistivity from south to north conforms to variations in lithological properties (e.g. texture and porosity). Southwardly, where alluvial materials are more dominant, low resistivity sediments are more prevalent, while in northern and northcentral regions, where coarse materials are more widespread, sediments are generally characterised by higher resistivities. High resistivity ( $> 50 \Omega\text{m}$ ) materials, whose lateral continuity is interrupted by moderately

low resistivity ( $\sim 10\text{--}25 \Omega\text{m}$ ) sediments, underlie the top-ping materials in ERT 3. The high resistivity materials are dominantly medium sands, which are common around the WDS, while the intervening low resistivity materials were interpreted to probably, be the electrical response of materials used in filling a deep gully that was latter converted to the present WDS. These materials are still exposed at some sections of the road. ERTs 1 and 2 are basally filled with moderately high resistivity ( $> 20 \Omega\text{m}$ ) fine-medium sands.

### Pattern of soil and water contaminations

Surficial sediments in Calabar, characterised by low–moderate–high resistivities, are nearly homogeneous in abundance and spread. The one- and two-dimensional subsurface models obtained from surface resistivity investigations and results obtained from geochemical analyses of soil and water resources compare favourably well with results reported by Edet and Okereke (2002) from stand-alone investigations. The import of these observations is that there have been

no significant changes in the conditions of soil and water resources in Calabar. However, at the WDS, the VES curves are distorted at shallow depths that were coincident with depth to low resistivity portions on the 2-D models from ERT. These distortions were interpreted to be indicative of contamination at shallow depths (Meju 2000; Kaya et al. 2007; Fernández et al. 2014). The contaminated areas are generally thin (> 5 m). The mean concentrations of chemical parameters in the contaminated areas are slightly altered even though in some cases, they are still within permissible limits.

Sediments in the superficial layers (upper 2–3 layers) in unaltered areas are also characterised by low–moderate–high resistivities. In the southern and flood plain areas, where argillites and alluvial sediments dominate the epithelial layers, SWLs are high and resistivities are low. But in the elevated northern areas, medium–very coarse sediments are more abundant and consequently, SWLs are low and resistivities are high. Thus, moisture (type and composition) and lithology appear to be the dominant factors controlling the resistivities of the sediments. The anomalous low resistivity zones observed in the WDS at shallow depth are contamination markers. The leachate-contaminated soils are characterised by elevated pH, TDS and other geochemical and geophysical parameters. The high values of EC and mobile ions (e.g.  $\text{Cl}^-$ ) prevalent in the leachates are indicators that they can be harmful to the environment (Bagchi 1987). Furthermore, the comparatively high pH observations in the leachates suggest that biochemically controlled exothermic reactions, which culminate in high residual temperatures of the leachates, take place under acetogenic conditions. However, the weakly acidic conditions of SWR and groundwater near the WDS reveal that the contaminations are strongly localised due to strongly attenuations.

The low–moderate resistivity (31.3–1973.5  $\Omega\text{m}$ ) character of thin (< 10 m) sediments in the upper layer, which, at the WDS, are underlain by comparatively low resistivity sediments, was attributed to the abundance of residual ions, metals and other substances deposited at the interface between the first and second layers by surface run-off and other percolating fluids. Although these processes can enhance the ionic concentration of the interfacial sediments, they deplete the epithelial layers of cementing materials like clay and silt, some common minerals, e.g. calcium, magnesium, nitrogen, phosphorous and potassium, and salt residues. Cumulatively, these depletions in the capping sediments, and ionic and mineral enhancements in the underlying sediments create sharp resistivity contrast, which was captured as abrupt break in the continuity of the VES curves (Meju 2000).

Comparatively, the distribution of ground resistivities and geochemical parameters of both subsurface and groundwater resources correlates strongly with the findings of Edet and

Worden (2009) every except at the WDS. This suggests that any evidence of contamination like in the WDS is a highly localised. This anomalous feature was, therefore, attributed to localised changes in type and composition of the pore fluid emanating from the WDS (Meju 2000).

## Conclusions

Results from integrated studies involving resistivity (VES and ERT) and geochemical analyses of soil, SWR, groundwater and textural analyses have been used in assessing the contamination levels of soil and water resources in Calabar. The various investigative tools adopted were directed at generating reasonably good contrasts in physical, geochemical and textural parameters between any contaminated area and other parts of Calabar. Results obtained are within the limits established by previous workers in the area indicating that there have been no reasonable changes in the physico-chemical properties of the soil and water resources in the area. However, at the WDS, where leachates generated by wastes at various stages of decomposition exist, results obtained were marginally higher. These show that the soils are locally contaminated mainly by leachates generated by decomposed materials in the WDS. The contaminated area is about 5 m in vertical extent while its lateral spread is negligibly low (< 3 m). This absence of reasonable continuity in the lateral spread of the contaminated area was attributed to strong attenuation of the leachates by the underlying and adjoining clayey and lateritic sediments. Additionally, the technical sloping of the WDS at  $\geq 20^\circ$  during its construction stage also helps in enhancing downslope flow of leachates at the expense of their vertical flow. This design helps in mitigating the extent of contamination. Finally, the results show that either there are no significant anthropic-borne contaminant generating activities going on in the area or wastes generated from such activities are adequately controlled.

Therefore, all monitoring, control and managing programmes currently being implemented by all waste management agencies should be sustained even when the present WDS is closed.

**Acknowledgements** The authors are grateful to the University of Calabar, Calabar, for providing the funds and facilities used in this study. In addition, contributions from students, who assisted at different data acquisition regimes, are thankfully acknowledged. Finally, the authors are grateful to the reviewers whose criticisms, suggestions and sometimes direct text editing help in improving the quality of the original manuscript.

## References

- Abidin MHZ, Madun A, Tajudin SAA et al (2017) Forensic assessment on near surface landslide using electrical resistivity imaging



- (ERI) at Kenyir Lake Area in Terengganu, Malaysia. *Procedia Eng* 171:434–444
- Akpan ER, Ekpe UJ, Ibok UJ (2002) Heavy metal trends in the Calabar River, Nigeria. *Environ Geol* 42:47–51
- Akpan AE, George NJ, George AM (2009) Geophysical investigation of some prominent gully erosion sites in Calabar, southeastern Nigeria and its implications to hazard prevention. *Disaster Adv* 2(3):46–50
- Akpan AE, Chidomerem TE, Akpan IO (2014a) Geophysical and laboratory studies of the spread and quality of the Odukpiani limestone deposit, southeastern Nigeria. *Am J Environ Sci* 10(4):347–356
- Akpan AE, Ebong ED, Ekwok SE et al (2014b) Geophysical and geological studies of the spread and industrial quality of Okurike barite deposit. *Am J Environ Sci* 10(6):569–577
- Alloway BJ (1990) Heavy metals in soils. Blackie Academic and Professional, London
- Almasri MN, Kaluarachchi JJ (2004) Assessment and management of long-term nitrate pollution of ground water in agriculture-dominated watersheds. *J Hydrol* 295:225–245
- Al-Tarazi E, El-Naqa A, El-Waheidi M et al (2006) Electrical geophysical and hydrogeological investigations of groundwater aquifers in Ruseifa municipal landfill, Jordan. *Environ Geol*. <https://doi.org/10.1007/s00254-006-0283-4>
- APHA (2005) Standard methods for the examination of water and wastewater, 21st edn. American Public Health Association, Washington
- Bagchi A (1987) Natural attenuation mechanisms of landfill leachate and effects of various factors on the mechanisms. *Waste Manag Res* 5(4):453–463
- Barte AG, Barifajjo E, Kiberu JM et al (2010) Correlation of geoelectric data with aquifer parameters to delineate the groundwater potential of hard rock terrain in central Uganda. *Pure appl Geophys* 167:1549–1559
- Bhattacharya P, Samal AC, Majundar J et al (2010) Arsenic contamination in rice, wheat, pulses, and vegetables: a study in an arsenic affected area of West Bengal, India. *Water Air Soil Pollut* 213(1–4):2–13
- Caputo R, Piscitelli S, Oliveto A et al (2003) High-resolution resistivity tomographies in active tectonic studies. Examples from the Tyrnavos Basin, Greece. *J Geodyn* 36:19–35
- Casas A, Himi M, Diaz Y et al (2008) Assessing aquifer vulnerability to pollutants by electrical resistivity tomography (ERT) at a nitrate vulnerable zone in NE Spain. *Environ Geol* 54:515–520
- CCME, Canadian Council of Ministers of the environment (1999) Canadian soil quality guidelines for the protection of environmental and human health. Canadian Environment Guidelines No. 1299. CCME, Winnipeg. ISBN 1-896997-34-1
- Chen TB, Wong JWC, Zhou HY et al (1999) Assessment of trace metal distribution and contamination in surface soils of Hong Kong. *Environ Pollut* 96(1):61–68
- Çolak M (2012) Heavy metal concentrations in sultana-cultivation soils and sultana raisins from Manisa (Turkey). *Environ Earth Sci* 67:695–712
- D'Amato G, Cecchi L, D'Amato M et al (2010) Urban air pollution and climate change as environmental risk factors of respiratory allergy: an Update. *J Investig Allergol Clin Immunol* 20(2):95–102
- Dang YP, Dalal RC, Mayer DG et al (2008) High subsoil chloride concentrations reduce soil water extraction and crop yield on Vertisols in north-eastern Australia. *Aust J Agric Res* 59:321–330
- Eckhardt DA, Stackelberg PE (1995) Relation of ground-water quality to land use on Long Island, New York. *Ground Water* 33(6):1019–1033
- Edet AE, Okereke CS (2002) Delineation of shallow groundwater aquifers in the coastal plain sands of Calabar area (Southern Nigeria) using surface resistivity and hydrogeological data. *J Afr Earth Sc* 35:433–443
- Edet AE, Worden RH (2009) Monitoring of the physical parameters and evaluation of the chemical composition of river and ground-water in Calabar (Southeastern Nigeria). *Environ Monit Assess* 157:243–258
- Edet AE, Merkel BJ, Offiong OE (2003) Trace element hydrochemical assessment of the Calabar coastal plain sand aquifer, southeastern Nigeria. *Environ Geol* 44:137–149
- Edet A, Ukpong A, Nganje T (2014) The concentration of potentially toxic elements and total hydrocarbon in soils of the Niger Delta Region (Nigeria). *J Environ Earth Sci* 4(1):23–34
- Fernández DS, Puchulu ME, Georgieff SM (2014) Identification and assessment of water pollution as a consequence of a leachate plume migration from a municipal landfill site (Tucumán, Argentina). *Environ Geochem Health* 36(3):489–503
- FPDD, Fertilizer Procurement and Distribution Division (1990) Literature review on soil fertility investigation in Nigeria, vol 1–5. Federal Ministry of Agriculture and Natural Resources, Lagos
- Gemal KS, El-Shishtawy AM, El-Alfy MM et al (2011) Assessment of aquifer vulnerability to industrial waste water using resistivity measurements. A case study along El-Gharbyia main drain, Nile Delta, Egypt. *J Appl Geophys* 75:140–150
- Gillis AC, Birch GF (2006) Investigation of anthropogenic trace metals in sediments of Lake Illawarra, New South Wales. *Aust J Earth Sci* 53:523–539
- Giocoli A, Quadrio B, Bellanova J et al (2013) Electrical resistivity tomography for studying liquefaction induced by the May 2012 Emilia-Romagna earthquake (Mw = 6.1, North Italy). *Nat Hazards Earth Syst Sci Discuss* 1:5545–5560
- Halihan T, Albano J, Comfort SD et al (2012) Electrical resistivity imaging of a permanganate injection during in situ treatment of RDX-contaminated groundwater. *Groundw Monit Remediat* 32:43–52
- Hargreaves JC, Adl MS, Warman PR (2008) A review of the use of composted municipal solid waste in agriculture. *Agric Ecosyst Environ* 123:1–14
- Heincke B, Günther T, Dalsegg E et al (2010) Combined three-dimensional electric and seismic tomography study on the Åknes rockslide in Western Norway. *J Appl Geophys* 70:292–306
- Hermans T, Vandenbohede A, Lebbe L et al (2012) A shallow geothermal experiment in a sandy aquifer monitored using electric resistivity tomography. *Geophysics* 77(1):B11–B21
- Iloje NP (2001) A new geography of Nigeria. New Revised Edition. Longman Nigeria PLC, Ibadan, p 200
- Islami N, Taib SH, Yusoff I et al (2011) Integrated geoelectrical resistivity, hydrochemical and soil property analysis methods to study shallow groundwater in the agriculture area, Machang, Malaysia. *Environ Earth Sci*. <https://doi.org/10.1007/s12665-011-1117-6>
- ISO 11277 (1998) Soil quality—determination of particle size distribution in mineral soil material—method by sieving and sedimentation. International Organization for Standardization, Geneva, Switzerland
- Jalali M (2010) Nitrate pollution of groundwater in Toyserkan, western Iran. *Environ Earth Sci*. <https://doi.org/10.1007/s12665-010-0576-5>
- Kanmani S, Gandhimathi R (2013) Assessment of heavy metal contamination in soil due to leachate migration from an open dumping site. *Appl Water Sci* 3(1):193–205
- Kaya MA, Özürlan G, Şengül E (2007) Delineation of soil and groundwater contamination using geophysical methods at a waste disposal site in Çanakkale, Turkey. *Environ Monit Assess* 135:441–446
- Kolachchi Z, Jalali M (2006) Effect of water quality on the leaching of potassium from sandy soil. *J Arid Environ* 68:624–639

- Krishna AK, Govil PK (2007) Soil contamination due to heavy metals from an industrial area of Surat, Gujarat, Western India. *Environ Monit Assess* 124:263–275
- Lee J-Y, Song S-H (2007) Evaluation of groundwater quality in Coastal Areas: implications for sustainable agriculture. *Environ Geol* 52:541–548
- Lehto M, Kuisma R, Määttä J et al (2011) Hygienic level and surface contamination in fresh-cut vegetable production plants. *Food Control* 22(3–4):469–475
- Loke MH (2004) Electrical imaging surveys for environmental and engineering studies: a practical guide to 2-D and 3-D surveys. [www.terraplus.com](http://www.terraplus.com). Date accessed 30 Oct 2015
- Loke MH, Barker RD (1996) Rapid least-squares inversion of apparent resistivity pseudosections using a quasi-Newton method. *Geophys Prospect* 44:131–152
- Loska K, Danutta W, Korus I (2004) Metal contamination of farming soils affected by industry. *Environ Int* 30(2):159–165
- Lowenberg U, Kunzel T (1991) Investigation on the trawl fishery of the Cross River estuary, Nigeria. *J Appl Ichthyol* 7:44–53
- MacFarlane DS, Cherry JA, Gillham RW et al (1983) Migration of contaminants in groundwater at a landfill: a case study: 1. Groundwater flow and plume delineation. *J Hydrol* 63:1–29
- Meju M (2000) Geoelectrical investigation of old/abandoned, covered landfill sites in urban areas: model development with a genetic diagnosis approach. *J Appl Geophys* 44:115–150
- Metcalf & Eddy, Burton FL, Stensel HD, Tchobanoglous G (2003) *Wastewater engineering: treatment and reuse*. McGraw Hill, Boston, p 59
- Meziani B, Machane D, Bendaoud A et al (2017) Geotechnical and geophysical characterization of the Bouira-Algiers Highway (Ain Turck, Algeria) landslide. *Arab J Geosci*. <https://doi.org/10.1007/s12517-017-2926-z>
- Mitrofan H, Povară I, Maftciu M (2007) Geoelectrical investigations by means of resistivity methods in karst areas in Romania. *Environ Geol* 55:405–413
- Neves MA, Morales N (2007) Structural control over well productivity in the Jundiá River Catchment, Southeastern Brazil. *An Acad Bras Ciênc* 79(2):307–320
- Nganje TN, Edet AE, Ekwere SJ (2007) Concentrations of heavy metals and hydrocarbons in groundwater near petrol stations and mechanic workshops in Calabar metropolis, southeastern Nigeria. *J Environ Geosci* 14(1):15–29
- Okoyeh EI, Akpan AE, Egboka BCE, Okeke HI (2013) An assessment of the influences of surface and subsurface water level dynamics in the development of gullies in Anambra State, southeastern Nigeria. *Earth Interact* 18:1–24
- Orellana E, Mooney AM (1966) Master curve and tables for vertical electrical sounding over layered structures. *Interciencia*, Madrid
- Orisakwe OE, Asomugha R, Afonne OJ et al (2004) Impact of effluents from a car battery manufacturing plant in Nigeria on water, soil and food qualities. *Arch Environ Health* 59(1):31–36
- Pánek T, Margielewski W, Tábořík P et al (2010) Gravitationally induced caves and other discontinuities detected by 2D electrical resistivity tomography: case studies from the Polish Flysch Carpathians. *Geomorphology* 123(1–2):165–180
- Pettyjohn WA (1971) Water pollution by oil-field brines and related industrial wastes in Ohio. *Ohio J Sci* 71:257
- Rao NS (2002) Geochemistry of groundwater in parts of Guntur district Andhra Pradesh, India. *Environ Geol* 41:552–562
- Rao NS (2006) Seasonal variation of groundwater quality in a part of Guntur district, Andhra Pradesh, India. *Environ Geol* 49:413–429
- Rao GT, Gurunadha Rao VVS, Padalu G et al (2014) Application of electrical resistivity tomography methods for delineation of groundwater contamination and potential zones. *Arab J Geosci* 7(4):1373–1384
- Reijers TJA, Petters SW (1987) Depositional environment and diagenesis of Albian carbonates in Calabar Flank, S. E. Nigeria. *J Petrol Geol* 10:283–294
- Reijers TJA, Petters SW, Nwajide CS (1987) The Niger Delta Basin. In: Selley RC (ed) *African basins—sedimentary basin of the world*, vol 3. Elsevier Science, Amsterdam, pp 151–172
- Réveillère A, Hamm V, Lesueur H et al (2013) Geothermal contribution to the energy mix of a heating network when using Aquifer Thermal Energy Storage: modeling and application to the Paris basin. *Geothermics* 47:69–79
- Revil A, Johnson TC, Finizola A (2010) Three-dimensional resistivity tomography of Vulcan's forge, Vulcano Island, southern Italy. *Geophys Res Lett* 37:L15308
- Rosales RM, Martínez-Pagan P, Faz A et al (2012) Environmental monitoring using electrical resistivity tomography (ERT) in the subsoil of three former petrol stations in SE Spain. *Water Air Pollut*. <https://doi.org/10.1007/s11270-012-1146-0>
- Sartelet KN, Couvidat F, Seigneur C et al (2012) Impact of biogenic emissions on air quality over Europe and North America. *Atmos Environ* 53:131–141. <https://doi.org/10.1016/j.atmosenv.2011.10.046>
- Scott RL, Edwards EA, Shuttleworth WJ et al (2004) Interannual and seasonal variation in fluxes of water and carbon dioxide from a riparian woodland ecosystem. *Agric For Meteorol* 122:65–84
- Singh KP (1994) Temporal changes in the chemical quality of ground water in Ludhiana area. *Curr Sci* 66:375–378
- Singh T, Karra YP (1975) Specific conductance method for in situ estimation of total dissolved solids. *J Am Water Works Assoc* 67(2):99–100
- Smith RC, Sjogren DB (2006) An evaluation of electrical resistivity imaging (ERI) in Quaternary sediments, Southern Alberta, Canada. *Geosphere* 2(6):287–298
- Srinivasamoorthy K, Chidambaram S, Prasanna MV et al (2008) Identification of major sources controlling groundwater chemistry from a hard rock terrain—a case study from Mettur Taluk, Salem District, Tamilnadu, India. *J Earth Syst Sci* 117(1):1–10
- Srinivasamoorthy K, Gopinath M, Chidambaram S et al (2014) Hydrochemical characterization and quality appraisal of groundwater from Pungar sub basin, Tamilnadu, India. *J King Saud Univ Sci* 26:37–52
- Sudha K, Israil M, Mittal S et al (2009) Soil characterization using electrical resistivity tomography and geotechnical investigations. *Appl Geophys* 67:74–79
- Sujatha B, Reddy BR (2003) Quality characterisation of groundwater in the south-eastern part of the Ranga Reddy District, Andhra Pradesh, India. *Environ Geol* 44:579–586
- Telford WM, Gildart LP, Sheriff RE (1990) *Applied geophysics*, 2nd edn. Cambridge University Press, Cambridge
- Van Niekerk H, Silberbauer MJ, Maluleke M (2014) Geographical differences in the relationship between total dissolved solids and electrical conductivity in South African rivers. *Water SA* 40(1):133–137
- Vender Velpen BPA (1988) A computer processing package for D.C. resistivity interpretation for an IBM compatibles. *ITC J* 4:1–4
- Wallin EL, Johnson TC, Greenwood WJ et al (2013) Imaging high stage river-water intrusion into a contaminated aquifer along a major river corridor using 2-D time-lapse surface electrical resistivity tomography. *Water Resour Res* 49(3):1693–1708
- Wilkinson PB, Meldrum PI, Kuras O et al (2010) High-resolution electrical resistivity tomography monitoring of a tracer test in a confined aquifer. *J Appl Geophys* 70:268–276
- World Health Organization (2004) *Guidelines for drinking water quality: incorporating first addendum: vol 1—recommendations*. WHO Publications, Geneva, Switzerland
- Yadav GS, Dasgupta AS, Sinha R et al (2010) Shallow sub-surface stratigraphy of interfluvies inferred from vertical electrical soundings

- in western Ganga Plains, India. *J Quat Int.* <https://doi.org/10.1016/j.quaint.2010.05.030>
- Yang SM, Li FN, Suo DR et al (2006) Effects of long-term fertilization on soil productivity and nitrate accumulation in Gansu Oasis. *Agric Sci China* 5(1):57–67
- Youdeowei PO, Nwankwoala HO (2010) Subsoil Characteristics and Hydrogeology of the Export Processing Zone, Calabar-Southeastern Nigeria. *J Appl Sci Environ Manag* 14(2):11–15
- Zhou W, Beck BF, Adams AL (2002) Effective electrode array in mapping karst hazards in electrical resistivity tomography. *Environ Geol* 42:922–928